Thermal and Structural Analysis of the ITER ELM Coils

A. W. Brooks[1], Y. Zhai[1], E. Daly[2], M. Kalish[1], R. Pillsbury[3], A. Khodak[1]

[1]Princeton Plasma Physics Lab, Princeton, NJ
[2]ITER Organization, Cadarache, France
[3]Sherbrooke Consulting, Arlington, VA
abrooks@pppl.gov

Abstract— **A thermal and structural analysis of the ELM Coil design for ITER is presented. The ELM Coils are constructed using a jacketed mineral insulated conductor of CuCrZr, MgO and Inconel 625, rigidly mounted to the vacuum vessel inner shell, behind the Blanket Modules. Since the coils are not designed to be remotely maintained, a major issue is demonstrating the structural integrity against fatigue and crack propagation over an estimated 100 million cycles arising from operation at 5 hz in a high magnetic field. The temperature rises from ohmic and nuclear heating produce mean thermal stresses that further limit the allowable alternating stresses. Thermal growth also imparts large forces which must be reacted by the Vacuum Vessel. This paper presents the analysis and results with particular attention to the design criteria which is unique to the In-Vessel Coils.**

Keywords—ELM Coil, ITER, Analysis

I. INTRODUCTION

The ELM Coils are an array of 27 coils fixed to the wall of the ITER Vacuum Vessel that generate resonant magnetic perturbations to control the plasma so that certain types of plasma instabilities called Edge-Localized Modes (ELMs) are avoided. The ELM Coils present a unique structural challenge in that they must operate for near infinite life (~100 million cycles) at ac currents in a high magnetic field and nuclear heating environment. The analysis must demonstrate they can function for the life of ITER without repair or replacement since they are inaccessible, inside the Vacuum Vessel (VV) and trapped behind the Blanket Shield Modules. This translates to designing to the fatigue stress endurance limit for all materials and assuring the stress intensity factor associated with crack propagation remains below the crack initiation threshold.
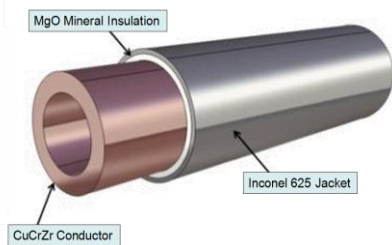

Figure 1 ELM Cable made from CuCrZr Conductor, MgO Insulation and Inconel 625 Jacket
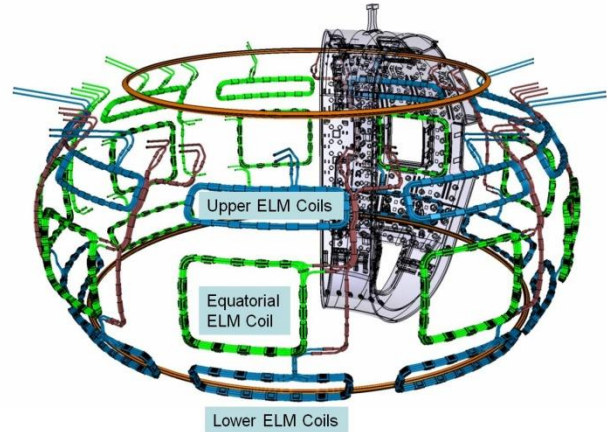
Figure 2 ITER ELM Coil Configuration

II. OVERVIEW OF DESIGN

The design of the ELM Coils is described in detail in [1]. The design has evolved to satisfy the driving requirement of near infinite life. Early designs attempted to use flexible supports that permitted thermal growth of the coils, resulting from ohmic and nuclear heating, and still withstand the large Lorentz forces. After many design iterations and refinement of design requirements the flexible supports were abandoned in favor of rigid supports.

A number of other changes were implemented to mitigate the impact of the increase in reaction loads on the vacuum vessel mounting rails from thermal growth of the coils. The conductor cross section area fraction and the cooling water hole area fraction were optimized within the available space to minimize temperature rises with an increased flow velocity of 8 m/s. The nuclear heating of the coils and supports was found in [2] to be lower than originally assumed further reducing temperature rises. The rails were modified in both number (more) and size (smaller) to better carry the loads. The jacket thickness was increase and change from 316 SS to Inconel 625 to increase the fatigue strength and allow for longer unsupported lengths of the cable where supports could not be accommodated in the design. This also allowed eliminating the central spine and further reduced the nuclear heating due to the reduced volume. The lower coefficient of thermal of Inconel 625 relative to the 316 SS vacuum vessel results in the coil being in tension prior to a pulse when at the same

temperature as the VV. But as the coil heats up during the pulse the tension is reduced before eventually going into compression. This reduces the maximum magnitude of stress in the coils and the reaction loads to the VV rails.

III. ANALYSIS DESCRIPTON

The thermal and structural analysis of the ELM coils described herein was performed using the ANSYS code. Additional analyses performed by others provided inputs such as nuclear heating [3] and disruption currents [4]. The geometry of the coils was defined by CATIA CAD models. The analysis presented focuses on the Equatorial ELM Coil (aka Mid ELM Coil) but similar analysis was done for the Upper ELM [5], Lower ELM (Y. Zhai) and Feeders (A. Khodak).

A. ANSYS Model

A finite element model of the CATIA geometry was created in ANSYS that was suitable for addressing the multiphysics environment. This includes the hydraulics and convective heat transfer of the cooling water, the ohmic heating from the electric current, the nuclear heating applied from the neutronics analysis, magnetic field calculations from the background field coils and plasma, Lorentz forces from the electromagnetic (EM) interactions and structural response.

Figure 3 shows the resulting model. The model consists mostly of a swept mesh except at the turn transition corner supports. The centerlines of the turns were extracted from the CAD geometry. The rail locations in the CAD models were used to segment the centerlines before importing for sweeping of the different sections.
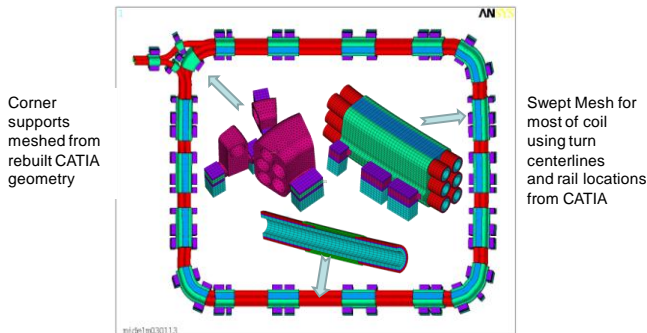

Figure 3 ANSYS Model of Equatorial ELM Coil. Similar modeling done for the Upper and Lower ELM Coils and Feeders
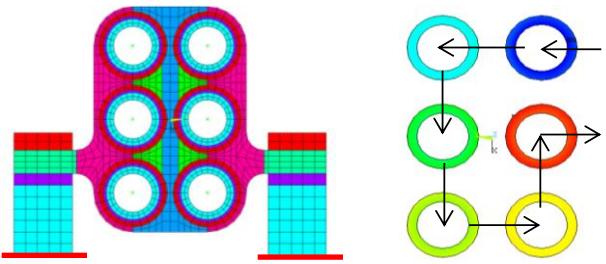

Figure 4 Section thru coil at supports (left) and thru conductor showing water flow pattern thru turns to minimize thermal gradients

Figure 4 shows a section thru one of the many supports in the model and a section thru the conductor showing the cooling water path thru the coil. Water enters the top turn, closest to plasma, which experiences the highest nuclear heating. This minimizes the thermal gradients from turn to turn. For the thermal analysis the water flow is modeled with FLUID116 elements that are convectively coupled to SURF152 elements overlaid on the SOLID90 conductor elements. The solid element types are change for the EM and structural analyses to SOLID5 and SOLID186 respectively.

B. Loads and Boundary Conditions

The coils are subject to a number of operating scenarios shown summarized in Table 1 below. They represent various time points during a DD or DT pulse.

Table 1 Loading Scenarios

			Current		Nuc Heat
Run#	Mode	State	Ohmic Heating, kA (rms)	EM Loads, kA (peak)	Nuc Heating***, Poloidal Leg MW/m3
1	DD - NO	Initial Warmup to 100 C, VV also at 100 C	0	0	0
2		Start of Flat Top - Coil Still Cold - EM Only	0	15	0
3		End of Flat Top - Coil Warm - EM + Th	10.6	15	0
4		End of Pulse - Th Only	10.6	0	0
5	DD - Disrupt	Disruption Currents w/Cold Coil	0	15*	0
6		Disruption Currents w/Warm Coil	10.6	15*	0
7	DD-DC	DC Operation without Nuclear Heating	15	15	0
8	DT - NO	Start of Pulse - Coil Cold, VV Warm (from Nuc Heat)	0	0	1.12
9		Start of Flat Top - Coil Still Cold - EM Only	0	15	1.12
10		End of Flat Top - Coil Warm - EM + Th	10.6	15	1.12
11		End of Pulse - Th Only	10.6	0	1.12
12	DT - Disrupt	Disruption Currents w/Cold Coil	0	15*	1.12
13		Disruption Currents w/Warm Coil	10.6	15*	1.12
14	DT-DC	DC Operation with Nuclear Heating	15	15	1.12
15	Bakeout	Bakeout to 200 C	0	0	0
16	Fault	No Water Cooling (Radiation and/or He Cooling)	0	0	1.12
17	Seismic	SL-1			
18		SL-2			

The initial warm-up to 100 C imposes a prestress due to the difference in thermal expansion of the coils and VV.

EM loading is based on the normal operating current of 15 kA at 5 hz with a background field from the PF Coils, TF Coils, Plasma Current and self fields. The end of burn was previously identified as producing the highest fields at the ELM coils.

Ohmic heating is based on the rms current of 10.6 kA. For the Mid ELM coils this produces a total of 240 kW.
The nuclear heating is based on a number of detailed 2D distributions provide in [2]. The heating is a maximum at

points closest to the plasma and drops off radially. Simple exponential fits were used to approximate the heating. For the Mid ELM, the poloidal legs have a peak value of 1.12 MW/m3 from leakage between the BMs while the toroidal legs see 0.86 MW/m3. The decay length was found to be 0.12 m.
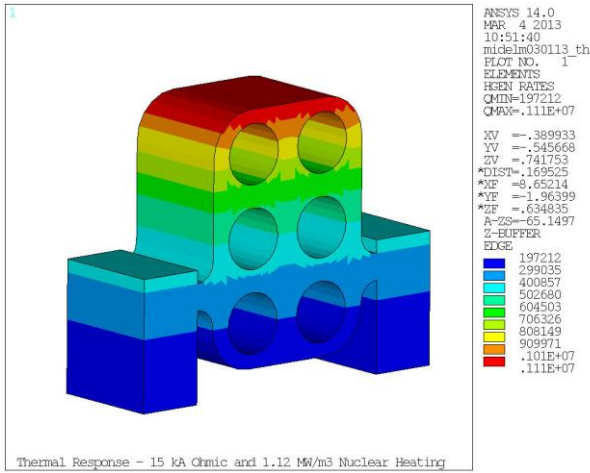

Figure 5 Nuclear heating distribution in poloidal leg of a Mid ELM Coil

Other load conditions include operating water pressure of 1.74 MPa and a static design pressure of 4 MPa. Disruption currents varied between coils. For the Mid and Lower ELM coils, the max induced currents were less than or equal to the normal operating current and were not analyzed explicitly. The number of design cycles for disruptions is also only ~1000 making them less severe than normal operation on coil life. The Upper ELM coil showed higher currents as discussed in [3]. Seismic loads on the coils are driven by the VV response to a seismic event. Accelerations were found to be on the order of 1g with excitation frequency driven by the natural frequency of the VV. The natural frequency of the coils was found to be an order of magnitude greater than the VV rendering the loads relatively insignificant.

Most of the heat generated or deposited into the coils is removed by the cooling water but some is conducted to the VV. A heat sink temperature of 119 C is imposed at the base of the rail/VV interface for normal operation with nuclear heating or 100 C without. An enforced displacement on the base of the rails is used to simulate the growth of the VV based on its average temperature of 110 C.

The brazed tubes are in good thermal and structural contact with the support brackets.

IV. ACCEPTANCE CRITERIA

There are many criteria that must be satisfied by the analysis as described in Appendix D to the Structural Design Criteria for ITER In-Vessel Components (SDC-IC). The ELM coil design is dominated by the need to meet the fatigue and crack growth criteria for the 100 million cycle design life. The static criteria for primary and secondary stresses are much less stringent.

To meet fatigue, it is necessary to show safety margins of 2 on stress and 20 on cycles. At 10^8 cycles we are at the endurance limit and allowable stresses are limited to half the endurance limit.

Crack propagation analysis typically considers regime B (or II) of a crack growth vs range of stress intensity factor curve as shown below.
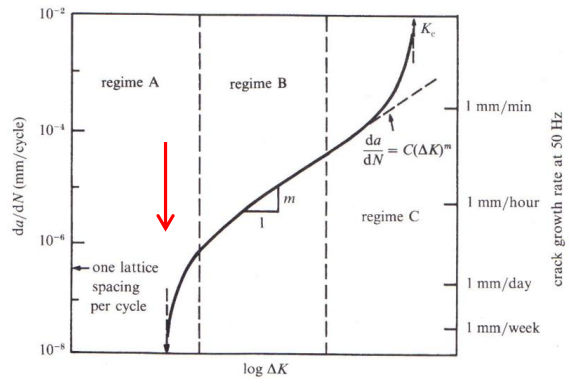

Fig. 10.8. Schematic illustration of the different regimes of stable fatigue crack propagation.

Figure 6 Typical crack growth behavior with the crack threshold highlighted

Once a crack starts to grow it has a limited life which is typically much less than 10^8 cycles. To meet near infinite life, the stress intensity factor must be less than the crack initiation threshold highlighted. This value is based on a detectable flaw size which has been assumed to be 0.3 mm^2.

Work done by Jun Feng [5] for this program allowed construction of allowable alternating stress range curves vs mean stress (somewhat analogous to the Goodman curve). This allowed incorporation of the crack initiation threshold criteria into ANSYS post processing scripts providing evaluation at all locations in a model. Similar post processing is used to evaluate fatigue based on SDC-IC
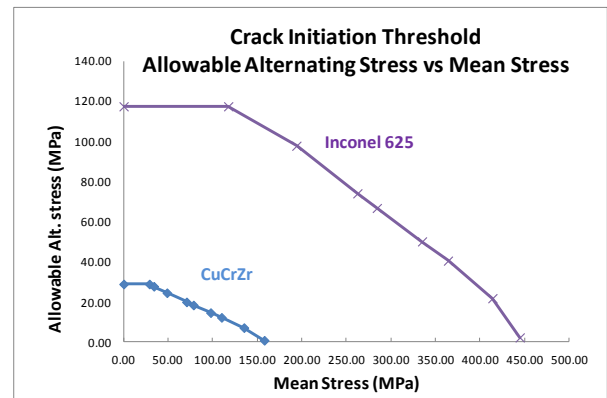

Figure 7 Crack Initiation Threshold calculated based on J Feng [6]

V. RESULTS

A. Thermal Response

There is 240 kW of dissipated power due to ohmic heating of the Mid ELM during normal operation at 15 kA ac (10.6 kA rms) and an additional 102 kW from nuclear heating. Most of this heat is removed by the water resulting in just over 12 C temperature rise. Less than 5 % is conducted to the VV. The peak temperature in the coil is due to conduction gradients induced by the nuclear heating. Figure 8 below shows the peak temperature occurring at a tall support at the leads. Excluding that peak, a max temperature of 200 C exists at the bolts.
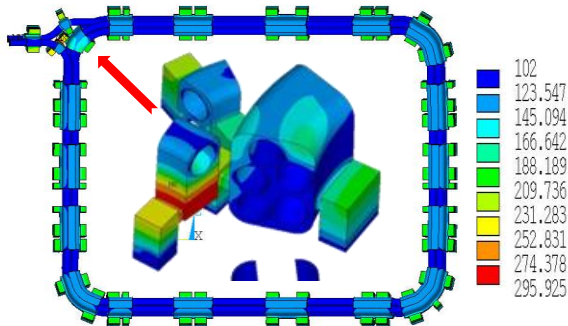

Figure 8 Temperature Response from Ohmic and Nuclear Heating

B. EM Fields and Forces

The EM forces are greatest on the poloidal leg, ~360 kN/m, due to the interaction of the 90 kA-turns with the 4 T TF field. The forces pull one leg away from the VV wall while pushing the opposite leg towards it. As the current reverses so do most of the forces – the exception being the self force component. The running loads on the longer toroidal legs which cross the PF field are about a factor of 4 smaller.
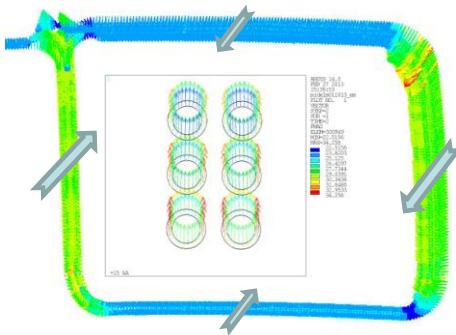

Figure Force Distribution on Mid ELM Coil During Normal Operation

C. Structural – Normal Operation

All load cases were simulated but only the Normal Operation Scenario results are shown below due to space limitations. Table 2 compares the results from a load cycle with the applicable criteria. The tabulated static criteria results for primary, primary local and secondary stress are actually the peak stresses found. Even so there are factors of ~5 on conductor stresses, ~3 on jacket stresses and close to two on

support stresses. The figures below are plots of the equivalent alternating stress defined in the criteria as the actual alternating tresca stress, S_{alt}, for the full load cycle adjusted for the mean stress, S_{mean}, of the cycle: $S_{eq} = S_{alt}/(1-S_{mean}/S_{ult})$ where S_{ult} is the ultimate tensile strength. The figures are generated for each component by post processing in ANSYS the extreme load cases for the cycle to compute S_{alt}, S_{mean} and S_{eq} (results of computation are stored in Ux for plotting).
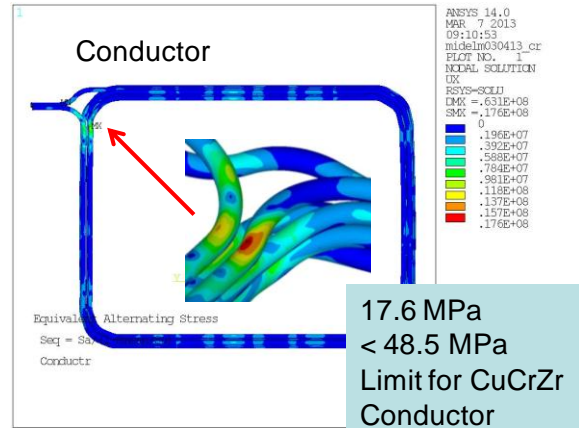

17.6 MPa
< 48.5 MPa
Limit for CuCrZr Conductor

Figure 9 Conductor Equivalent Alternating Stress

80.6 MPa
< 200. MPa
Limit for Inco 625 Jacket

Figure 10 Jacket Equivalent Alternating Stress

158 MPa
< 200. MPa
Limit for Inco 625 Support Brackets
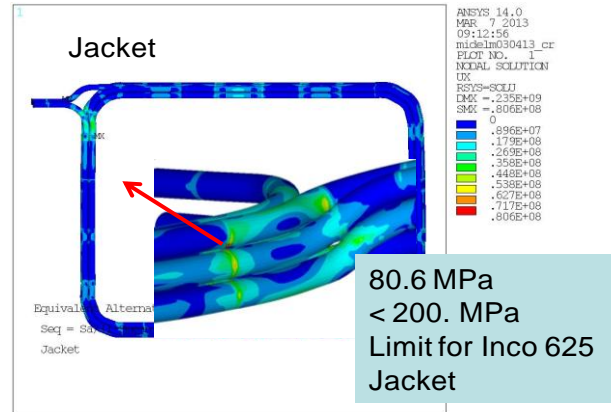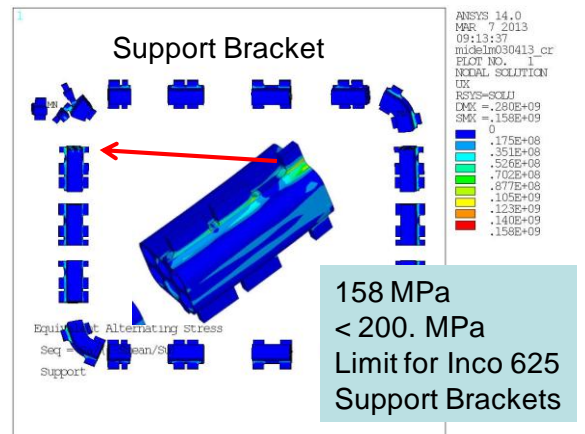
Figure 11 Supports Equivalent Alternating Stress

Table 2 Summary of Stress Results for Normal Operation with Ohmic and Nuclear Heating

Criteria			Conductor, CuCrZr		Jacket, Inco625		Supports, Inco625	
			Limit	+/- EM + Nuc + Ohmic	Limit	+/- EM + Nuc + Ohmic	Limit	+/- EM + Nuc + Ohmic
Static Stress	Primary*		120	20.8	276	78.8	276	139
(Tresca)	Local Primary	EM	180	20.8	414	78.8	414	139
	Secondary	Thermal+EM	360	50.9	827	159	827	523
		Thermal-EM	360	52.5	827	188	827	457
		Mean	360	**51.7**	827	168	827	477
Fatigue			48.5	17.6	200	80.6	200	158
(Equivalent Alternating Tresca)								
Crack Threshold Margin (-Good, +Bad)			0	-35	0	-98.9	0	-5.28
(Tensile Range of Principle Stress, Kth=15)								

These results for normal operation with alternating EM loads from +/-15 kA and max temperature rises from ohmic and full nuclear heating were actually not the worst case found. Because of the differences in thermal coefficient of expansion, there is a greater relative thermal strain between the coil and the VV at the start of a pulse when the coil is still cold. While the alternating stresses from EM do not change, the mean stresses and resulting equivalent stresses increase. This produces what appears to be excessive stress based on the linear global model results. They are relieved when nonlinear behavior at the bolted joint is included in the analysis.
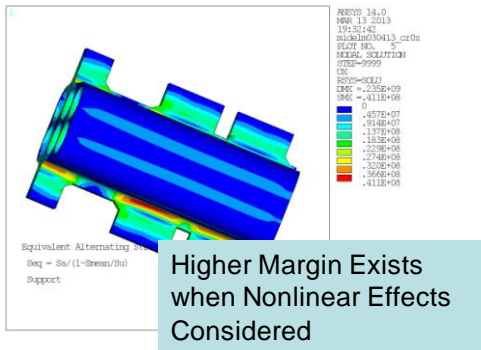

Higher Margin Exists when Nonlinear Effects Considered

Figure 12

D. Bakeout

The mismatch in thermal coefficients of expansion between the 316 SS VV and the Inconel Jacket & Support, while beneficial for Normal Operation, can result in higher stresses and reaction loads during bakeout if the coil and VV are at the same temperature.

Increasing the coil bakeout temperature to 240 C by using the same system as the BM reduces this significantly. Figure 13 shows the impact of bakeout temperature on the max rail reaction load. There is a fairly broad range of bakeout temperatures which will lead to lower rail reaction loads than are predicted for normal operation.
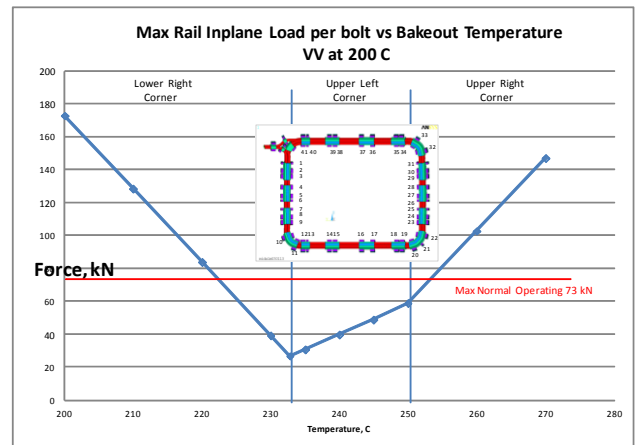

Figure 13

E. Faulted Coil

If a coil were to fail due to water leak and/or an electrical short it would have to remain in place without unduly jeopardizing machine operation. A small leak may be repairable in-situ permitting helium cooling with reduced operation. A larger leak means coil cooling must rely on radiation and conduction only, significantly increasing re-cool time. In either case the cooling is not very effective during a 500s pulse and relies on the 1300s between pulses (i.e. 1800s rep rate). Temperature rises of over 100 C will overstress the VV rails and/or cause slippage at the bolted joints. The number of cycles tolerable will be reduced based on the strain range in the 316 SS Rails. Many more cycles would be tolerable with shorter pulses.
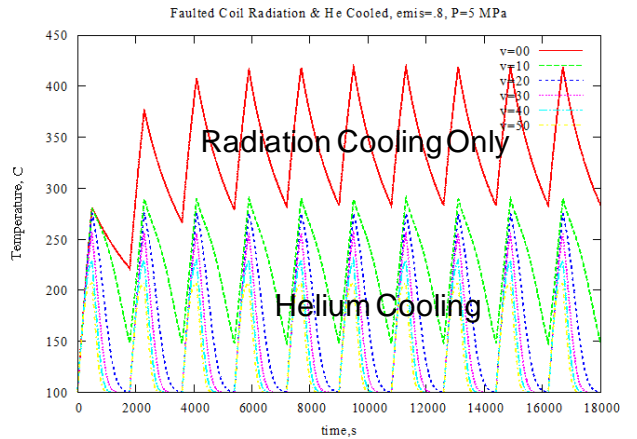

Figure 14 Faulted coil pulsed at full power for 500s followed by 1300s cool down.

An elastic-plastic analysis was performed on the global ANSYS model of the Mid ELM. Results showed that the coil and support brackets remain elastic except in a few localized regions. The corner rails, which must carry the bulk of the thermal load, yield. The displacements and rotations of the worse case rail from the global model were applied to a local 2D model. The 316 SS yields as shown in Figure 15. A strain

criteria is used in this case to determine the number of cycles the structure can last.

The corner rail shown below on a faulted foil can survive ~300 pulses at full 500 s each (max temperature ~226C, average 175 C). For a 250s pulses, the strain is only 0.33% and expected life increases to 10,000 cycles. Bolt slippage may occur before rail strains are reached further limiting strain range and possibly increasing life.
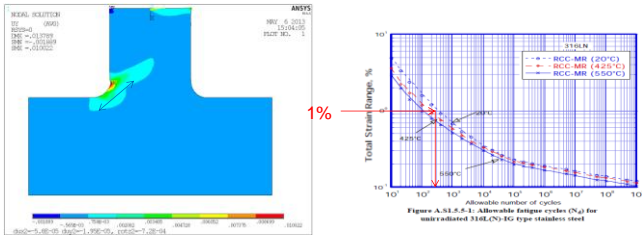

Figure 15

VI. CONCLUSIONS

The analysis results presented herein show the design meets all applicable criteria for all operating scenarios analyzed. The high cycle life demanded is achievable. Bakeout at 240 results in acceptable stresses (ie using the Blanket Module water system as opposed to the VV water system). Seismic, disruption and DC operation were identified as being less severe than the Normal Operation scenarios. Conductor Stresses from 4 MPa design pressure are well within the static criteria for the CuCrZr. A faulted coil could limit the life of the VV rail supports or impose limits on pulse length to minimize heating.

REFERENCES

[1] M. Kalish "Design Analysis and Manufacturing Studies for ITER In-Vessel Coils", 2013 SOFE Conference Proceedings

[2] M. Sawan, "Model and Analysis of Results_for_BM15_65T6DK_v1 0", dated 02/15/2012

[3] R. Pillsbury, "Final Report on the ELM and VS Coil Design ITER Task Number: C15TD70FU", dated May, 2011

[4] Shanwen Zhang, "Mechanical analysis of the ITER Upper ELM Coil", 2013 SOFE Conference Proceedings

[5] J. Feng, "Estimation of Allowable Stress by using the threshold concept", internal memo dated 05/20/2011